



Research Article



## Synthesis and characterization of Titanium dioxide nanoparticles and nanocomposites with CdS

Sumalatha Donthula<sup>1</sup> and Jagadeesh Kumar Ega<sup>2</sup>

### Corresponding Author:

[jkjadeeshkumare@gmail.com](mailto:jkjadeeshkumare@gmail.com)

### DOI:

<http://dx.doi.org/>

10.17812/IJRA.3.11(81)2016

### Manuscript:

Received: 19<sup>th</sup> July, 2016

Accepted: 16<sup>th</sup> Aug, 2016

Published: 30<sup>th</sup> Sep, 2016

### Publisher:

Global Science Publishing  
Group, USA

<http://www.globalsciencepg.org/>

### ABSTRACT

Transition metal oxides possess fundamental and technological properties due to the influence of many

factors such as the presence of d-electrons, crystalline structure, oxygen defects and doped impurities. In view of this work, abundant efforts have been attempted to improve charge separation by modifying the surface or bulk properties of TiO<sub>2</sub>, such as doping, deposition of metals, size reduction and coupling of two semiconductors and thereby improving the photo catalytic activity. Nanocrystal line TiO<sub>2</sub> has unique physico-chemical, optical and electronic properties, excellent pigmentary properties, high ultraviolet absorption and high stability which allow it to be used in biomedical coatings, electro ceramics, self-cleaning surface coating and building materials. Titanium dioxide nanoparticles and nanocomposites elemental studies were carried out using Fourier Transform Infrared Spectroscopy (FTIR) and Energy Dispersive X-ray Spectroscopy (or EDS). Diffraction studies were carried out using X-Ray Diffraction (XRD) Spectroscopy. Microscopic studies were performed by Scanning Electron Microscope and Transmission Electron Microscope. The TGA curve revealed high thermal stability of the synthesized nanoparticles, absence of any impurity or intermediate complex and high melting point.

**Keywords:** Titanium dioxide, Nano composites, FTIR, EDS, XRD and TGA

### IJRA - Year of 2016 Transactions:

Month: July-September

Volume – 3, Issue – 11, Page No's:487-493

Subject Stream: Chemistry

**Paper Communication:** Author Direct

**Paper Reference Id:** IJRA-2016: 3(11)487-493



## Synthesis and characterization of Titanium dioxide nanoparticles and nanocomposites with CdS

Sumalatha Donthula<sup>1</sup> and Jagadeesh Kumar Ega<sup>2</sup>

### ABSTRACT

Transition metal oxides possess attracting fundamental and technological properties due to the influence of many factors such as the presence of d-electrons, crystalline structure, oxygen defects and doped impurities. In view of this work, abundant efforts have been attempted to improve charge separation by modifying the surface or bulk properties of TiO<sub>2</sub>, such as doping, deposition of metals, size reduction and coupling of two semiconductors and thereby improving the photo catalytic activity. Nanocrystalline TiO<sub>2</sub> has unique physico-chemical, optical and electronic properties, excellent pigmentary properties, high ultraviolet absorption and high stability which allow it to be used in biomedical coatings, electro ceramics, self-cleaning surface coating and building materials. Titanium dioxide nanoparticles and nanocomposites elemental studies were carried out using Fourier Transform Infrared Spectroscopy (FTIR) and Energy Dispersive X-ray Spectroscopy (or EDS). Diffraction studies were carried out using X-Ray Diffraction (XRD) Spectroscopy. Microscopic studies were performed by Scanning Electron Microscope and Transmission Electron Microscope. The TGA curve revealed high thermal stability of the synthesized nanoparticles, absence of any impurity or intermediate complex and high melting point.

**Keywords:** Titanium dioxide, Nano composites, FTIR, EDS, XRD and TGA.

### 1. INTRODUCTION

Titanium dioxide (TiO<sub>2</sub>) belongs to one of these prototypes. Titanium dioxide itself has no d-electron, but the number of d-electron can be controlled by doping<sup>1</sup>. In addition to the wide bandgap, TiO<sub>2</sub> exhibits many other interesting properties, such as transparency to visible light, high refractive index, and low absorption coefficient<sup>2</sup>. It is inexpensive, chemically stable and non-toxic. TiO<sub>2</sub> has been used since ancient times as white pigments. It possesses white color because it has no absorption in the visible region<sup>3</sup>. The importance of TiO<sub>2</sub> as photocatalyst for splitting of water was first highlighted by Honda and Fujishima<sup>4,5</sup>, since then due to its unique electronic, optoelectronic, Photo catalytic Water Decomposition, Cleaning Building Materials and modified Sol–Gel Process<sup>6-11</sup>. TiO<sub>2</sub>, is an important IV-VI group semiconductor (SC<sup>12</sup>, and can

crystallize in three polymorphic forms with Photo catalytic Property of Bicrystalline TiO<sub>2</sub>/Rectorite Composites.<sup>13,14</sup> It gives a representative diagram of structures of different TiO<sub>2</sub> phases. In its pure form TiO<sub>2</sub> is an n-type semiconductor with indirect band gaps of 3.2eV (387nm) for anatase, 3.02eV (410nm) for rutile and 3.25eV (381nm) for brookite<sup>15</sup>, between the filled oxygen 2p valence band (VB) and titanium 3d states at the bottom of the conduction band (CB). All these crystalline structures of TiO<sub>2</sub>, consist of deformed TiO<sub>6</sub> octahedron, connected differently by corners and edges. Among these forms, anatase and rutile are most common whereas brookite, is uncommon and unstable<sup>16</sup>. Rutile is the most stable form, whereas anatase and brookite are metastable forms and can readily transform to rutile on heating<sup>17</sup>. The temperature at which anatase to rutile transformation takes place varies from 400°C to 1000°C depending on concentration of

impurities in the crystals or annealing atmosphere<sup>18</sup>.

White pigment in paints, food coloring, toothpastes, cosmetics<sup>19-27</sup>, in environmental friendly method for air purification<sup>28</sup>, flexible dye-sensitized solar cells<sup>29</sup>, humidity sensors<sup>30</sup>, electrochromic devices, photovoltaic fuel cells, and above all as photo catalyst for air and water purification and also for water splitting to produce H<sub>2</sub>. Diffraction (XRD) Spectroscopy, Scanning Electron Microscopy (SEM) and Transmission Electron Microscopy (TEM). TiO<sub>2</sub> NP absorbs light at <385nm leading to excitation of electrons (e<sup>-</sup>) from the valence band to the conduction band, leaving behind a positively charged vacancy called a hole (h<sup>+</sup>). The hole by itself is a very powerful oxidizing agent and may lead to the generation of hydroxyl radicals in presence of water and molecular oxygen or can directly oxidize adsorbed species on NP surface. TiO<sub>2</sub> has an advantage of having a capability to perform function using sunlight as an energy source. These photo induced charges have very short lifetime due to charge recombination, releasing the absorbed light energy as heat, with no chemical effect. Therefore, it is important to prevent electron-hole recombination in order to improve the efficiency and efficacy of TiO<sub>2</sub>. Also TiO<sub>2</sub> can only effectively absorb in UV region of the solar spectrum which makes up only about 5% of the total solar energy that falls on the earth's surface, thus limiting its use.

## 2. MATERIALS AND METHODS

Synthetic technique for TiO<sub>2</sub> nanoparticles involved controlled precipitation of nanoparticles from precursors dissolved in a solution. Here, a simple method was proposed for the synthesis of TiO<sub>2</sub> nanoparticles from the reductive hydrolysis of Titanium Tetra Isopropoxide (TTIP) in methanol at ambient temperature and pressure without calcinations. A series of TiO<sub>2</sub> NP (**Tma**, **Tmb**, **Tmc**, **Tmd** and **Tme**) was synthesized by varying the concentration of TTIP and keeping the amount of methanol (24.44M) constant at 100mL. The concentration of TTIP varies as; for **Tma**=0.25M, **Tmb**=0.20M, **Tmc**=0.15M, **Tmd**=0.1M and **Tme**=0.05M. The reactions proceeded as; 100mL methanol (24.44M) was taken in a conical flask and TTIP was added to it drop wise (20

drops per minute) while vigorous stirring, which was continued for additional 5 hours. White precipitates were obtained, which were washed with water and acetone several times and then air dried. In a reaction vessel 100mL aqueous Cd(NO<sub>3</sub>)<sub>2</sub>(0.085M) was taken and 50mL methanol (24.44M) was added drop wise with continuous stirring. The reaction was then carried out in H<sub>2</sub>S atmosphere for 1 minute with vigorous stirring, which was continued for 2 hours. The solution turned transparent to yellow. To this solution 3.53mL TTIP (0.1M) was added drop-wise (20 drops per minute). Stirring was continued to additional 5 hours. The solution turned to light yellow in color. The synthesized TiO<sub>2</sub> NP and CdS-TiO<sub>2</sub> NC were characterized by various techniques.

## 3. RESULTS AND DISCUSSION

The white colored fine powders were obtained as a result of reductive hydrolysis of TTIP suggesting the formation of TiO<sub>2</sub> nanoparticles. **Figure 4.2** shows the as-synthesized TiO<sub>2</sub> nanoparticles in suspension form, and **Figure 4.3** shows them in dried form. The synthesized TiO<sub>2</sub> having a mixture of anatase, brookite and rutile crystal structure was expected. For CdS-TiO<sub>2</sub> the color of the sample was yellow.

### *Fourier Transform Infrared Spectroscopy (FTIR) Spectroscopy:*

The FTIR spectra confirmed the purity and composition of the samples as several peaks related to TiO<sub>2</sub> were observed in all samples without any other elemental impurity. The bands for Ti-O and Ti-O-Ti bonds were present in the 800-400 cm<sup>-1</sup> region. The FTIR spectra of TiO<sub>2</sub> might be in the form of broad band centered at 400-800 cm<sup>-1</sup> attributed to the vibration of Ti-O bonds in the TiO<sub>2</sub> lattice or as peaks centered at 760 cm<sup>-1</sup>, 680 cm<sup>-1</sup>, 600 cm<sup>-1</sup>, 560 cm<sup>-1</sup>, 500 cm<sup>-1</sup>, 468 cm<sup>-1</sup>, 410 cm<sup>-1</sup>, 385 cm<sup>-1</sup> and 350 cm<sup>-1</sup> assigned to the (Ti-O-Ti) stretching vibration. **Figure 4.4** shows the FTIR spectra of the synthesized TiO<sub>2</sub> nanoparticles and its nanocomposites with CdS (**CdS-TiO<sub>2</sub>**). In the present case the FTIR spectra of TiO<sub>2</sub> NPs and **CdS-TiO<sub>2</sub>** NC was in the form of broad peak in the region 400-800 cm<sup>-1</sup> with several small peaks in it. The broad peak appearing at 3100-3600 cm<sup>-1</sup> was assigned to vibrations of hydroxyl groups of water

adsorbed by the samples. The weak absorption band at 1620-1630  $\text{cm}^{-1}$  was attributed to  $\text{CO}_2$  adsorbed on the surface of the particles. As it is known that adsorption of water and  $\text{CO}_2$  are common for all powder samples exposed to atmosphere and are even more pronounced for nanosized particles with high surface area. In case of  $\text{CdS-TiO}_2$ , the formation of CdS was confirmed by the appearance of peak at 405  $\text{cm}^{-1}$  assigned for Cd-S bond, and the presence of broad band centered at 400-800  $\text{cm}^{-1}$  with several small peaks in it confirms the presence of  $\text{TiO}_2$  in the nanocomposite. **Figure 4.5** contains the EDS spectra of the synthesized nanoparticles. The EDS spectra showed the presence of Ti and O peaks confirming the formation of pure  $\text{TiO}_2$  with no other elemental impurity for the samples **Tma**, **Tmb**, **Tmc**, **Tmd** and **Tme**. Other peaks in this figure corresponded to oxygen, carbon and silicate were due to sputter coating of glass substrate on the EDS stage and were not considered. The EDS spectra of  $\text{CdS-TiO}_2$  showed the presence of peak corresponded to Cd and S along with the peaks of Ti and O, thus confirming the formation of  $\text{CdS-TiO}_2$  nanocomposite.

#### *X-Ray Diffraction (XRD) Spectroscopy:*

X-ray diffraction patterns for  $\text{TiO}_2$  NPs were of rather poor quality due to the physical nature of the samples. However, the XRD pattern (**Figure 4.6**) of the synthesized  $\text{TiO}_2$  NPs revealed the presence of mixtures of anatase, brookite and rutile. The **Figure 4.6**, shows the peaks corresponded to anatase at  $2\theta = 25.56^\circ$  (101),  $37.8^\circ$  (103),  $48.07^\circ$  (200),  $54.18^\circ$  (105),  $62.42^\circ$  (204) and  $75.2^\circ$  (215), rutile at  $2\theta = 27.01^\circ$  (110),  $36.14^\circ$  (101),  $42.121^\circ$  (111),  $54.89^\circ$  (211) and  $68.72^\circ$  (301) and brookite at  $2\theta = 30.9^\circ$  (121) thus confirming the presence of mixed crystal phase. The estimated crystallite size for  $\text{TiO}_2$  samples (**Tma**, **Tmb**, **Tmc**, **Tmd** and **Tme**) based on the X-ray diffraction peak was not possible due to the presence of mixed peaks of anatase, rutile and brookite  $\text{TiO}_2$ .

**Figure 4.7** shows the XRD pattern of  $\text{CdS-TiO}_2$  nanocomposites, the pattern revealed the formation of cubic CdS and anatase  $\text{TiO}_2$  nanoparticles. The presence of peaks corresponded only to anatase  $\text{TiO}_2$  at  $2\theta = 25.56^\circ$  (101),  $37.282^\circ$  (103),  $48.07^\circ$  (200),  $54.18^\circ$  (105),  $62.42^\circ$  (204), was related to the formation of anatase  $\text{TiO}_2$

in  $\text{CdS-TiO}_2$ , while the formation of cubic CdS was confirmed by the presence of peaks corresponded only to cubic CdS at  $2\theta = 26.719^\circ$  (111),  $29.900^\circ$  (200),  $43.000^\circ$  (220),  $51.061^\circ$  (311).

#### *Scanning Electron Microscopy (SEM):*

The SEM micrographs showed the formation of well-defined spherical mesoporous  $\text{TiO}_2$  nanoclusters which were attributed to the high surface energy of nanosized  $\text{TiO}_2$  particles. **Figure 4.8 (a-e)**, shows the SEM images of the synthesized  $\text{TiO}_2$  NP above 7000 times magnification (7kx). **Figure 4.8 (f)** shows the SEM images of the synthesized  $\text{CdS-TiO}_2$  NC at 9000 times magnification (9kx). X-ray diffraction peak was not possible due to the presence of mixed peaks of cubic CdS and anatase  $\text{TiO}_2$ .

#### *Transmission Electron Microscopy (TEM):*

The TEM micrograph (**Figure 4.9 (a-f)**) of  $\text{TiO}_2$  NP (**Tma**, **Tmb**, **Tmc**, **Tmd** and **Tme**) showed the formation of spherical nanoclusters comprised of very small sized  $\text{TiO}_2$  NPs (1-2nm). The images showed a decrease in size of the nanocluster from  $>500\text{nm}$  (**Tma**) to  $<50\text{nm}$  (**Tme**). But the sizes of the individual  $\text{TiO}_2$  nanoparticles were less than 2nm in all the cases. For  $\text{CdS-TiO}_2$  the TEM image (**Figure 4.10**) confirmed the presence of both CdS and  $\text{TiO}_2$  nanoparticles. This was in good agreement with the EDS and XRD results.

#### *Thermal Gravimetric Analysis (TGA):*

The synthesized  $\text{TiO}_2$  NPs (**Tma**, **Tmb**, **Tmc**, **Tmd** and **Tme**) and  $\text{CdS-TiO}_2$  NC were found to be thermally stable upto temperature as high as  $1000^\circ\text{C}$  with a small weight loss at around  $100^\circ\text{C}$ , which was probably due to the presence of moisture and other volatile solvents. **Figure 4.11** shows the TGA results of synthesized  $\text{TiO}_2$  nanoparticles (**Tma**, **Tmb**, **Tmc**, **Tmd** and **Tme**) and  $\text{CdS-TiO}_2$  nanocomposite.

## 4. CONCLUSION

A series of Titanium Dioxide nanoparticles (**Tma**, **Tmb**, **Tmc**, **Tmd** and **Tme**) were successfully synthesized via single pot chemical precipitation method under ambient conditions. The synthesized  $\text{TiO}_2$  NP clearly showed that as the concentration of the Ti precursor decreased the size of the  $\text{TiO}_2$  nanocluster also decreased. The

size of the individual TiO<sub>2</sub> particle was not much affected. The synthesized NP showed good elemental purity without any contamination and good thermal stability. A mixed crystalline phase was observed in all TiO<sub>2</sub> samples. The micrographic studies revealed the formation of spherical clusters whose sizes decreased dramatically as the concentration of the Ti precursor decreased.

**Figure 4.1** The synthesized TiO<sub>2</sub>nanoparticles (Tma,Tmb,Tmc,TmdandTme) obtained as such in suspension form.

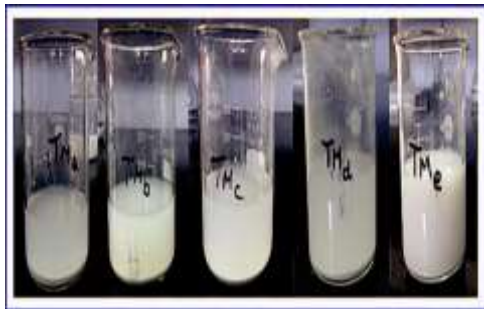


**Figure 4.2** The synthesized TiO<sub>2</sub>nanoparticles (Tma,Tmb,Tmc,TmdandTme) obtained after washing and drying.



**Figure 4.3** The FTIR Spectra of the synthesized TiO<sub>2</sub>nanoparticles (Tma,Tmb, Tmc,TmdandTme) and its nanocomposites with CdS (CdS-TiO<sub>2</sub>).

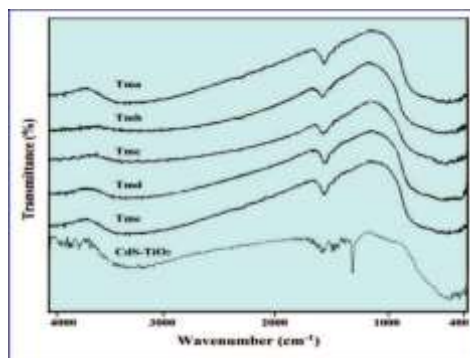


**Figure 4.4** EDS of the synthesized TiO<sub>2</sub>nanoparticles (Tma,Tmb,Tmc,Tmdand Tme) and its nanocomposites with CdS (CdS-TiO<sub>2</sub>).

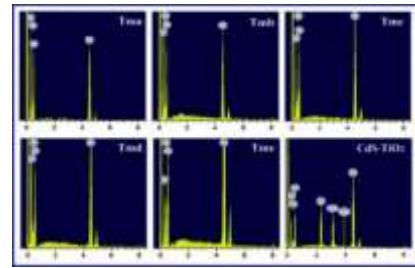


**Figure 4.6** XRD spectra of synthesized TiO<sub>2</sub>nanoparticles (Tm a, Tm b, Tm c, Tm d and Tm e).

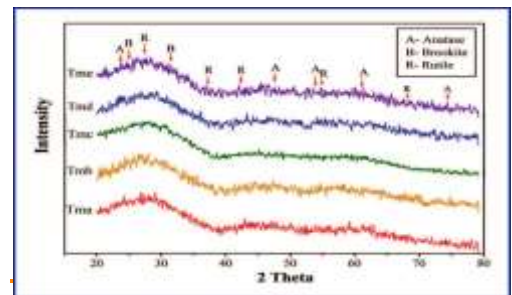


**Figure 4.7** XRD spectra of CdS-TiO<sub>2</sub> nanocomposites in comparison to pure cubicCdS and Degussa P-25 TiO<sub>2</sub>

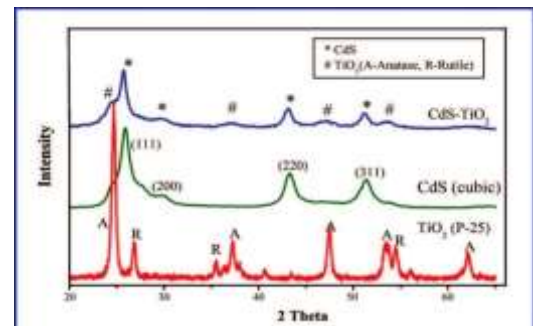


**Figure 4.8** SEM images (a) Tm a, (b) Tm b, (c) Tm c, (d) Tm d, (e) Tm e and (f) CdS-TiO<sub>2</sub>.

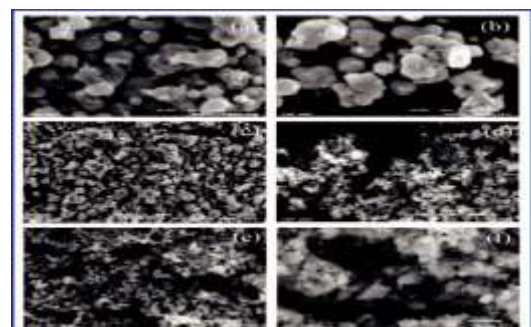


**Figure 4.9** TEM images of (a)Tma, (b)Tmb, (c)Tmc, (d) magnified portion of Tmc, (e)Tmd, (f)Tme, and in the inset are the magnified portion of the corresponding images.

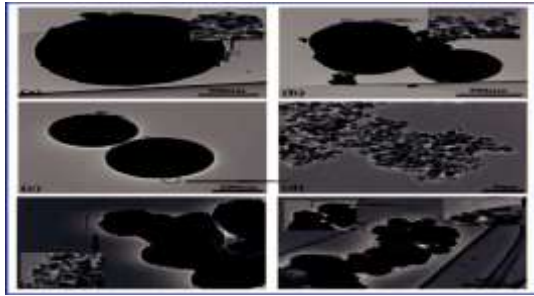


**Figure 4.10** (a), shows two different sized nanoparticles, the smaller were TiO<sub>2</sub> and the larger CdS nanoparticles. **Figure 4.10** (b), shows the representative diagram of CdS-TiO<sub>2</sub>. The particle

sizes obtained by TEM are listed in **Table 4.2**.

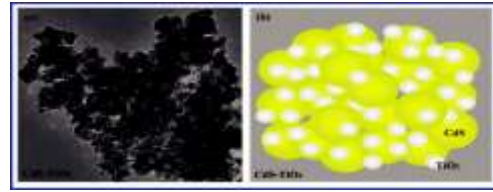


**Figure 4.11** TGA results of synthesized TiO<sub>2</sub>nanoparticles (Tm a, Tm b, Tm c, Tm d and Tm e) and CdS-TiO<sub>2</sub>nanocomposite

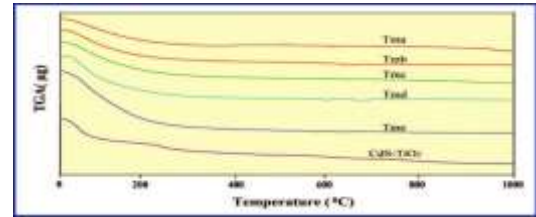


**Table 4.1** The explanation of the various peaks obtained by the FTIR spectra of the synthesized TiO<sub>2</sub> nanoparticles (Tm a, Tm b, Tm c, Tm d and Tm e) and CdS-TiO<sub>2</sub>.

Peak	Region	Intensity	Significance
A	400-420	Small and weak	Cd-S bond (CdS nanoparticles)
B	400-800	broad band	Ti-O bond vibration (TiO <sub>2</sub> nanoparticles)
C	570-620	Small and weak	S-S bond (crystal S-S bond)
D	1380-1420	Sharp or Broad	C-H bending of CH <sub>3</sub> (Acetone)
E	1620-1740	Small and weak	CO <sub>2</sub> bending or C-H bending (Acetone)
F	3140-3470	Broad	Intermolecular H-bonds (Lattice water)

**Table 4.2:** Average particle sizes of the synthesized TiO<sub>2</sub>NP (Tm a, Tm b, Tm c, Tm d and Tm e) and CdS-TiO<sub>2</sub>NC obtained by TEM

Nanoparticles	Tma	Tmb	Tmc	Tmd	Tme	CdS-TiO <sub>2</sub>
Particle Size (nm)	1.5-2.0	1.5-1.6	1.2-1.5	1-1.2	0.8-1.0	5-6 (CdS), 1.5-2 (TiO <sub>2</sub> )

## REFERENCES

- 1) Zhao, Y.; Zhang, X.; Zhai, J.; He, J.; Jiang, L.; Liu, Z.; Nishimoto, S.; Murakami, T.; Fujishima, A.; Zhu, D.: Enhanced Photocatalytic Activity of Hierarchically Micro-/Nano-Porous TiO<sub>2</sub> Films. *Applied Catalysis B: Environmental* 2008, 83, 24-29.
- 2) Richards, R.: *Surface and Nanomolecular Catalysis*; CRC/Taylor & Francis Boca Raton, FL, U.S.A., 2006.
- 3) Hashimoto, K.; Irie, H.; Fujishima, A.: TiO<sub>2</sub> Photocatalysis: A Historical Overview and Future Prospects. *Japanese Journal of Applied Physics* 2005, 44, 8269-8285.
- 4) Fujishima, A.; Honda, K.: Photolysis-Decomposition of Water at the Surface of an Irradiated Semiconductor. *Nature* 1972, 238, 37-38.
- 5) Linsebigler, A. L.; Lu, G.; Jr, J. T. Y.: Photocatalysis on TiO<sub>2</sub> Surfaces: Principles, Mechanisms, and Selected Results. *Chemical Reviews* 1995, 95, 735-758.
- 6) Girginer, B.; Galli, G.; Chiellini, E.; Bicak, N.: Preparation of Stable CdS Nanoparticles in Aqueous Medium and their Hydrogen Generation Efficiencies in Photolysis of Water. *International Journal of Hydrogen Energy* 2009, 34, 1176-1184.
- 7) Zhang, Y. J.; Yan, W.; Wu, Y. P.; Wang, Z. H.: Synthesis of TiO<sub>2</sub> Nanotubes Coupled with CdS Nanoparticles and Production of Hydrogen by Photocatalytic Water Decomposition. *Materials Letters* 2008, 62, 3846-3848.
- 8) Pichot, F.; Pitts, J. R.; Gregg, B. A.: Low-Temperature Sintering of TiO<sub>2</sub> Colloids: Application to Flexible Dye-Sensitized Solar Cells. *Langmuir* 2000, 16, 5626-5630.
- 9) Benedix, R.; Dehn, F.; Quaas, J.; Orgass, M.: Application of Titanium Dioxide Photocatalysis to Create Self-Cleaning Building Materials. *Lacer* 2000, 5, 157-168.
- 10) Li, Y.; Li, X.; Li, J.; Yin, J.: Photocatalytic Degradation of Methyl Orange by TiO<sub>2</sub> Coated Activated Carbon and Kinetic Study. *Water Research* 2006, 40, 1119-1126.
- 11) Wongkalasin, P.; Chavadej, S.; Sreethawong, T.: Photocatalytic Degradation of Mixed Azo Dyes in Aqueous Wastewater Using Mesoporous-Assembled TiO<sub>2</sub> Nanocrystal Synthesized by a Modified Sol-Gel Process. *Colloids and Surfaces A: Physicochemical and Engineering Aspects* 2011, 384, 519-528.
- 12) Maurya, A.; Chauhan, P.: Structural and Optical Characterization of CdS/TiO<sub>2</sub> Nanocomposite. *Semiconductors, Materials Characterization* 2011, 62, 382-390.
- 13) Ohno, K.; Tanaka, M.; Takeda, J.; Kawazoe, Y.: *Advances in Materials Research, Nano- and Micromaterials*; Springer Berlin Heidelberg New York, 2008; Vol. 9.
- 14) Zhang, Y.; Deng, L.; Zhang, G.; Gan, H.: Facile Synthesis and Photocatalytic Property of Bicrystalline TiO<sub>2</sub>/Rectorite Composites. *Colloids and Surfaces A: Physicochemical and Engineering Aspects* 2011, 384, 137-144.
- 15) Paola, A. D.; Cufalo, G.; Addamo, M.; Bellardita, M.; Campostrini, R.; Ischia, M.; Ceccato, R.; Palmisano, L.: Photocatalytic Activity of Nanocrystalline TiO<sub>2</sub> Powders Prepared by Thermohydrolysis of TiCl<sub>4</sub> in Aqueous Chloride Solutions. *Colloids and Surfaces A: Physicochemical and Engineering Aspects* 2008, 317, 366-376.
- 16) Al-Rasheed, R. A.: Water Treatment by Heterogeneous Photocatalysis: An Overview. In *4th SWCC Acquired Experience Symposium, Jeddah*. 2005.
- 17) Hanaor, D. A. H.; Sorrell, C. C.: Review of the Anatase to Rutile Phase Transformation. *Journal of Materials Science* 2011, 46, 855-874.
- 18) Shannon, R. D.; Pask, J. A.: Kinetics of the Anatase Rutile Transformation. *Journal of the American Ceramic Society* 1965, 48, 391-398.
- 19) Monticone, S.; Tufeu, R.; Kanaev, A. V.; Scolan, E.; Sanchez, C.: Quantum Size Effect in TiO<sub>2</sub> Nanoparticles: Does it exist? *Applied Surface Science* 2000, 162, 565-570.
- 20) Satoh, N.; Nakashima, T.; Kamikura, K.; Yamamoto, K.: Quantum Size Effect in TiO<sub>2</sub> Nanoparticles Prepared by Finely Controlled Metal Assembly on Dendrimer Templates. *Nature Nanotechnology* 2008, 3, 106-111.
- 21) Serpone, N.; Lawless, D.; Khairutdinov, R.: Size Effects on the Photophysical Properties of Colloidal Anatase TiO<sub>2</sub> Particles: Size Quantization versus Direct Transitions in this Indirect Semiconductor? *The Journal of Physical Chemistry* 1995, 99, 16646-16654.
- 22) Beranek, R.; Kisch, H.: Tuning the Optical and Photoelectrochemical Properties of Surface-Modified TiO<sub>2</sub>. *Photochemical & Photobiological Sciences* 2008, 7, 40-48.

- 23) Michael, A. H.: A Surface Science Perspective on TiO<sub>2</sub> Photocatalysis. *Surface Science Reports* 2011, 66, 185-297.
- 24) Roy, P.; Berger, S.; Schmuki, P. TiO<sub>2</sub> Nanotubes: Synthesis and Applications. *Angewandte Chemie International Edition* 2011, 50, 2904-2939.
- 25) Beeldens, A.: An Environmental Friendly Solution for Air Purification and Self-Cleaning Effect: The Application of TiO<sub>2</sub> As Photocatalyst in Concrete. In *Proceedings of Transport Research Arena Europe-TRA, Göteborg, Sweden, 2006*.
- 26) Ramakrishnan, R.; Sudha, J. D.; Reena, V. L.: Nanostructured Polyaniline-Polytitanate-Clay Composite for Photocatalytic Applications: Preparation and Properties. *RSC Advances* 2012, 2, 6228-6236.
- 27) Patel, A.; Prajapati, P.; Boghra, R.: Overview on Application of Nanoparticles in Cosmetics. *Asian Journal of Pharmaceutical Sciences and Clinical Research* 2011, 1, 40-45.
- 28) Reijnders, L.: Hazard Reduction for the Application of Titania Nanoparticles in Environmental Technology. *Journal of Hazardous Materials* 2008, 152, 440-445.
- 29) Dürr, M.; Schmid, A.; Obermaier, M.; Rosselli, S.; Yasuda, A.; Nelles, G.: Low-Temperature Fabrication of Dye-Sensitized Solar Cells by Transfer of Composite Porous Layers. *Nature Materials* 2005, 4, 607-611.
- 30) Wang, G.; Wang, Q.; Lu, W.; Li, J.: Photoelectrochemical Study on Charge Transfer Properties of TiO<sub>2</sub>-B Nanowires with an Application as Humidity Sensors. *The Journal of Physical Chemistry B* 2006, 110, 22029-22034.